

ZTF LED calibration analysis

Philippe Rosnet and Mickael Rigault

Laboratoire de Physique Clermont, CNRS/IN2P3 & Université Clermont Auvergne

Abstract

This note describes a first analysis of LED calibration flat fields with the three ZTF filters, based on a serie of runs recorded in September 2018. Detailed analysis of flat field images highlights several optical effects depending on filter-band. The wavelength response of each filter-band is studied and compared to basic expectation from measured LED spectra and filter transmission. Finally, pixels affected by diffuse light in LED flat fields are roughly identified.

Contents

1	LED calibration	2
2	Camera response to LED	3
2.1	Out of bandwidth effects	5
2.2	Within bandwidth effects	6
3	Wavelength dependence of filters	7
4	Cleaned LED flat field images	9
	References	10

1 LED calibration

The ZTF camera response can be studied with the help of calibrated LED's, either out or within each filter-band. The principle consists in illuminating the white dome with LED's reflecting a diffuse light with the aim to produce as much as possible a flat field. The serie of available LED's is shown in Fig. 1. Spectra represented with a full-line are the LED's used in this analysis (data with other LED's were not recorded). All spectra are normalized to have their maximum equal to one. Table 1 gives the two main characteristics of each LED spectrum: the peak wavelength (at maximum of the spectrum) and the integral of the spectrum (with the considered normalization).

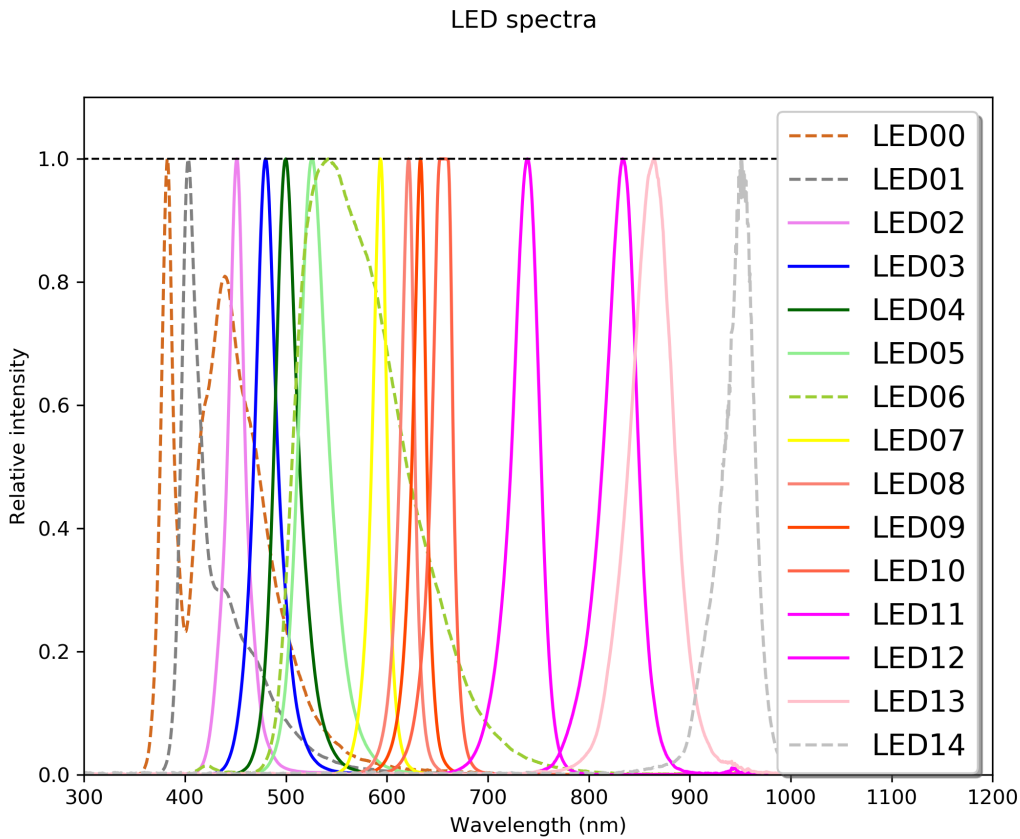


Figure 1: Spectra of LED's available for the calibration of the ZTF camera. All spectra are normalized to have their maximum equal to one. Full-line spectra show LED's used in this analysis.

The set of LED spectra can be compared to the three ZTF filter-bands, as shown in Fig. 2. For each filter, the full-line represents the measured transmission curve at 0^0 on center of the filter, while the rectangle is a simple modeling of the filter-band in term of two parameters: the mean transmission coefficient in the transmission band

Table 1: Main characteristics of LED's used in this analysis.

LED #	Peak wavelength (nm)	Spectrum integral (a.u.)
02	451.4	53.41
03	479.8	66.61
04	499.9	69.22
05	525.9	85.31
07	593.5	44.12
08	621.4	43.04
09	633.1	42.60
10	652.9	60.20
11	739.4	79.94
12	833.6	100.0
13	864.6	126.8

and the width of the transmission band defined at transmission equal to 0.5. Those modeling parameters are summarized in table 2

Table 2: Simple model parameters of filters in term of in-band mean transmission coefficient \bar{T} and bandwidth $\Delta\lambda$ defined by wavelengths at $T = 0.5$.

Filter ID	\bar{T}	$\Delta\lambda$ (nm)
G	0.911	[414.5 ; 546.2]
R	0.952	[565.6 ; 721.1]
I	0.997	[721.0 ; 873.2]

The LED calibration runs presented in this note were recorded the 10/09/2018 and consist in 2 seconds exposure to a single LED (thin full-line LED's of Fig. 1). Data are missing for a quarter (the upper right) of the camera. So, results concerns only the three other quarters of the focal plane.

2 Camera response to LED

For each filter, the camera response was studied independantly with each LED illumination to address the wavelength dependence. The full camera image was reconstructed using a two step procedure using the `numpy.concatenate` method:

1. A quadrant merging to form a CCD with each quadrant in the right position and orientation

```
# Rotation of each quadrant
q1 = np.rot90(fits.getdata(imgFilename, 1), 2)
```

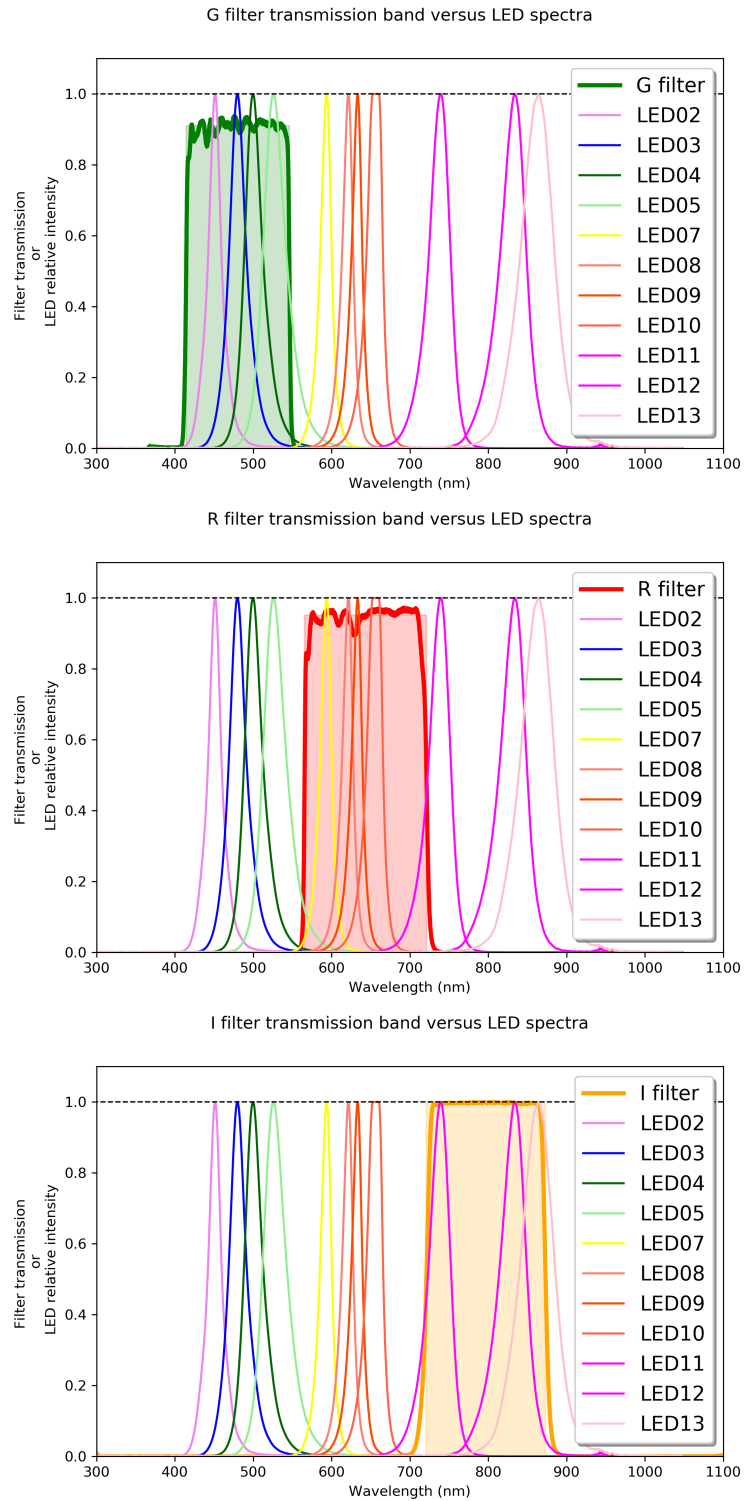


Figure 2: Filter-band transmission compared to LED's: upper pplot for G-filter, middle plot for R-filter and lower plot for I-filter.

```

q2 = np.rot90(fits.getdata(imgFilename, 2), 2)
q3 = np.rot90(fits.getdata(imgFilename, 3), 2)
q4 = np.rot90(fits.getdata(imgFilename, 4), 2)
# Horizontal merging of CCD quadrants Q1 and Q2
ccdUp = np.concatenate((q2, q1), axis=1)
# Horizontal merging of CCD quadrants Q3 and Q4
ccdDown = np.concatenate((q3, q4), axis=1)
# Vertical merging of the two above half-CCD
ccd = np.concatenate((ccdDown, ccdUp), axis=0)

```

2. The merging of all quadrants to form the full camera image

```

# Horizontal merging of CCDs line-per-line
line1 = np.concatenate((ccd[3], ccd[2], ccd[1], ccd[0]), axis=1)
line2 = np.concatenate((ccd[7], ccd[6], ccd[5], ccd[4]), axis=1)
line3 = np.concatenate((ccd[11], ccd[10], ccd[9], ccd[8]),
axis=1)
line4 = np.concatenate((ccd[15], ccd[14], ccd[13], ccd[12]),
axis=1)
# Vertical merging of the four CCD's lines to form the mosaic
focal_plane = np.concatenate((line1, line2, line3, line4),
axis=0)

```

The camera response for each filter and one LED out or within bandwidth is shown in Fig. 8 and 9 for filter G, in Fig. 10 and 11 for filter R, and in Fig. 12 and 13 for filter I. From those figures, we can note different visual effects on images depending on the LED is out or within bandwidth.

2.1 Out of bandwidth effects

For LED's out of bandwidth two mains effects can be reported.

1. A relative uniform counting of the focal plane with a clear quadrant-to-quadrant and CCD-to-CCD difference due to the amplification tuning of each quadrant electronics.
2. A spot on left and right edges of the full image between CCD lines 1 (3) and 2 (4). Those sopt are attributed to reflection of diffuse light on ($2k \times 2k$) CCD's on the perimeter of the mosaic used as guider, tip, tilt and focus [1], as shown in Fig. 3. This spot effect is seen only with filter G and R, but not with filter I. The difference comes from the size of the filter, with I covering the camera and the perimeter CCD's, while G and R filters cover only the camera, so light reflection on perimeter CCD's can contaminate the image. This problem is typically due

to diffuse light and is not expected during sky observation for which the light is more or less perpendicular to the focal plane.

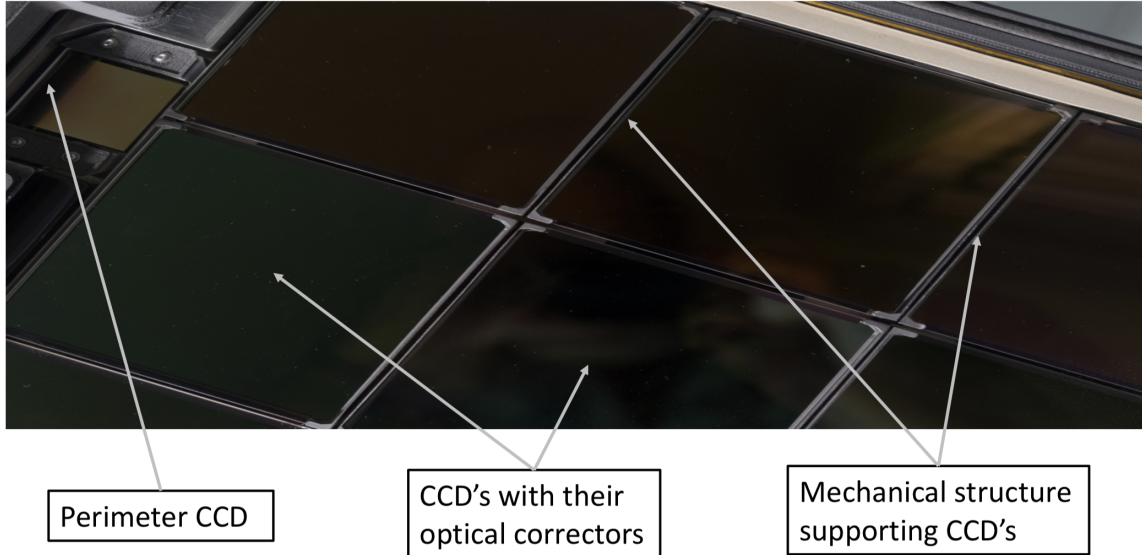


Figure 3: Camera view highlighting the perimeter CCD's and the mechanical structure supporting the CCD's.

2.2 Within bandwidth effects

For LED's within bandwidth five artefacts are clearly visible beyond the quadrant-to-quadrant and CCD-to-CCD amplitude differences.

1. The field-of-view limitation due to the entrance lens of the Schmidt telescope draws a large circle aperture effect.
2. Some specks (more or less large) are visible at same positions with the three filters, suggesting that their origin is common and certainly due to some dust inside the camera.
3. Nearly horizontal fringes are visible with filter G, but not with other filters. Figure 5 shows the Y-pixel profile of CCD 11, i.e. the relative response of Y-pixels on center of the CCD as a function the Y-pixel position. The fringes are characterized with a relative peak-to-peak amplitude of about 0.5% and a focal plane period of 256 pixels.
4. A tree-like structure at larger scale than horizontal fringes are visible with I filter.

5. Vertical spot lines are also visible with the three filters between CCD's. Figure 5 shows the X-pixel profile for CCD 11, i.e. the relative response of Y-pixel on center of the CCD as a function the X-pixel position. Reflection on edges of the CCD extends over about 100 pixels on each left and right sides with a maximum relative amplitude of about +5%. The origin of those spot lines seems to be due to diffuse lighth reflection on the mechanical structure supporting the CCD's, as shown on Fig. 3. As for edge spots, this problem is typically due to diffuse light and is not expected during sky observation where the lighth is more or less perpendicular to the focal plane.

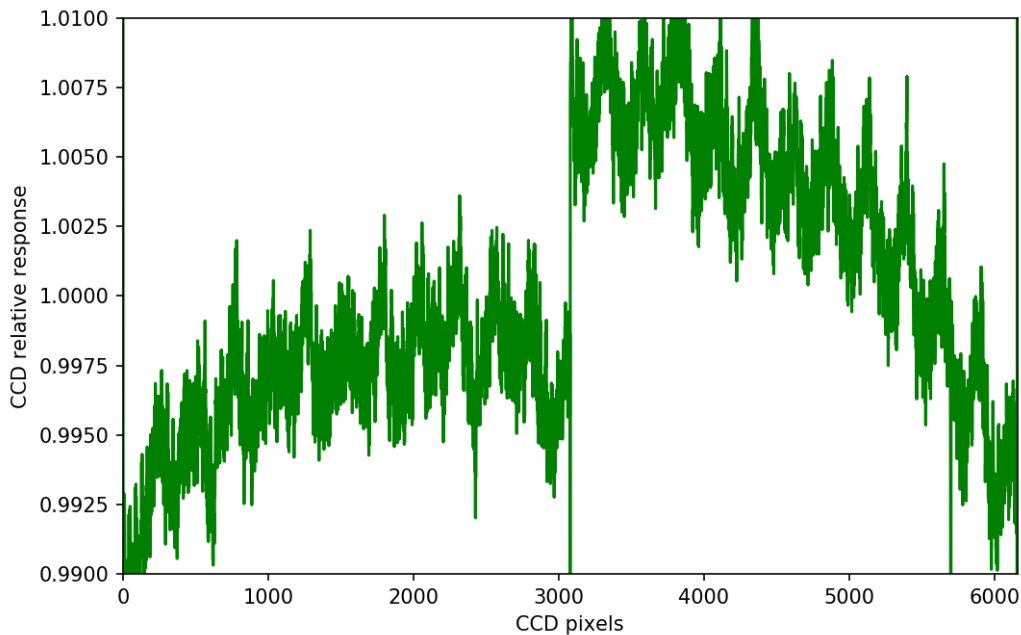


Figure 4: Y-pixel profile on center of CCD 11 with G filter illuminated with LED 03. The y -axis corresponds to the relative response computed as the mean relative counting of 20 adajacent X-pixel on the center of the CCD (10 pixels for each left and right quadrants) with the same Y-pixel position corresponding to the x -axis.

3 Wavelength dependence of filters

The study of the wavelegnth dependence of each filter is done by computing the mean counting of the focale plane for each LED $\langle N_{\text{count}}^{\text{LED}} \rangle$ normalized to a common factor chosen arbitrarily to 2^{16} . This normalization factor is chosen because the maximum of counting oberved for those LED runs is about 50,000, and that 2^{16} corresponds to the saturation level of a 16-bit encoding.

$$f_{\text{count}}^{\text{LED}} = \frac{\langle N_{\text{count}}^{\text{LED}} \rangle}{2^{16}}. \quad (1)$$

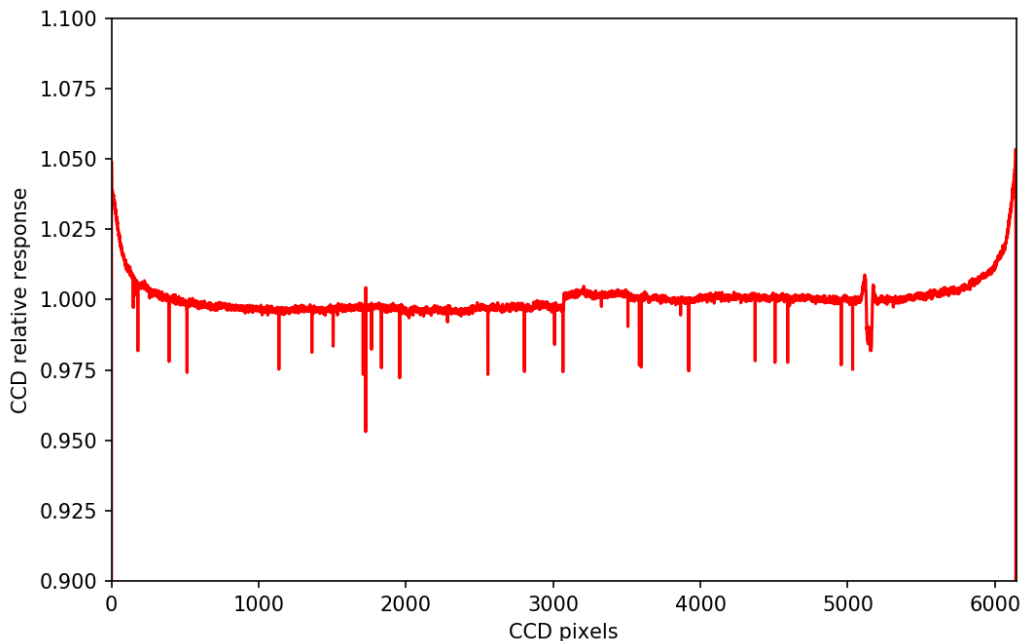


Figure 5: X-pixel profile on center of CCD 11 with R filter illuminated with LED 09. The y -axis corresponds to the relative response computed as the mean relative counting of 20 adjacent Y-pixels on the center of the CCD (10 pixels for each lower and upper quadrants) with the same X-pixel position corresponding to the x -axis.

LED "off" runs were recorded with R filter (LED "off" means LED intensity put to about its minimum, perhaps not completely turned off). Figure 6 shows the mean response of the full focal plane (counting normalized) as a function of the peak wavelength of each LED. The mean counting is constant over the full wavelength range. This flat behaviour suggests that the LED "off" counting has a non optical origin, like electronics or thermal noise. With the used normalization, the relative LED "off" counting is of the order of 10^{-3} .

For LED "on" runs, the mean focal plane relative counting $f_{\text{count}}^{\text{LED}}$ is compared to the expected fraction of light of the corresponding LED within the filter-band under study by computing the LED spectrum $I_{\text{LED}}(\lambda)$ convoluted with the filter transmission $T_{\text{filter}}(\lambda)$ normalized to the LED spectrum integral

$$f_{\text{filter}}^{\text{LED}} = \frac{\int I_{\text{LED}}(\lambda)T_{\text{filter}}(\lambda)d\lambda}{\int I_{\text{LED}}(\lambda)d\lambda}. \quad (2)$$

The simple modeling of filter-bands was used, i.e. their rectangle representation with parameters of table 2, to compute the expected fraction of LED light inside filter-bands. Results obtained for each filter are shown in Fig. 7. From this figure, we observe that the simple filter modeling reproduces the main behaviours of the filter transmission, but a full transmission curve is required to improve the matching. For LED out of bandwidth, the LED "off" level is observed with LED "on", and this level

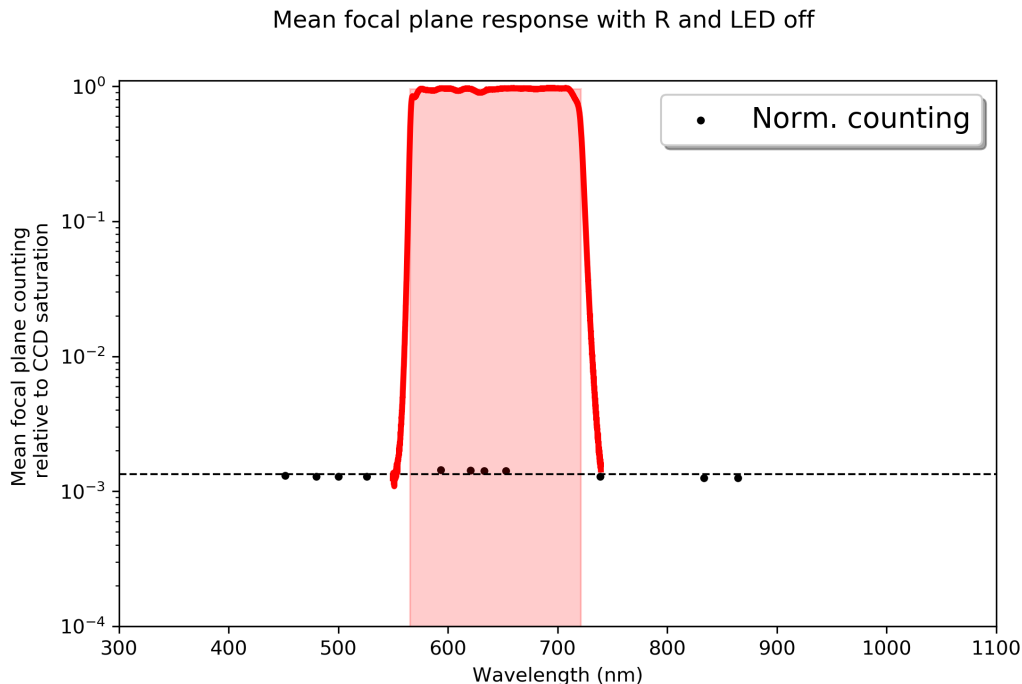


Figure 6: Normalized (to 2^{16}) mean focal plane counting (black points) with R filter as a function of the LED peak wavelength, for LED "off". The R filter transmission (red line) as well as its simple modeling (light-red rectangle) are shown.

is well reproduced by the computed fraction of light. This result suggests that the used arbitrary normalization (2^{16}) to compute the mean focal plane relative counting corresponds to a good approximated normalization factor.

4 Cleaned LED flat field images

Abnormal pixels can be defined as pixels affected by diffuse light effects. From previous discussion, two effects can be attributed essentially to diffuse light: (i) the spot edges only visible for light out of bandwidth for G and R filters and (ii) the vertical lines along the edges of each CCD. So, to be useful, the LED calibration runs must be cleaned of those effects. First, affected pixels can be identified by applying a threshold cut to the pixel counting compared to the mean value. As the mean value is dependent of each quadrant amplification, the mean value $\langle N_Q \rangle$ is computed for each quadrant (Q), as well as the associated standard deviation σ_Q . Then, for each quadrant the threshold cut to remove affected pixels is such that

$$N_{\text{count}} > \langle N_Q \rangle + n\sigma_Q. \quad (3)$$

- **Out of bandwidth** — A $n = 3$ cut is required to avoid to remove "noisy" pixels for out of bandwidth LED runs. This cut is optimized using LED out of

bandwidth run with I filter where the spot edges effect is absent. The results of pixel maps are presented in Fig. 14 for G filter, Fig. 16 for R filter and Fig. 18 for I filter.

- **Within bandwidth** — In this case, there is no "reference" run, and the cut level is optimized by visual testing. The choice of $n = 2$ seems to highlight vertical lines effects. The resulting pixel maps are shown in Fig. 15 for G filter, Fig. 17 for R filter and Fig. 19 for I filter. It can be noticed that with this cut, horizontal lines at the border of CCD's are also removed, but only between CCD line 1 (3) and 2 (4). The border line between CCD line 2 and 3 is not affected.

References

- [1] E.C. Belm et al., *The Zwicky Transient Facility: System Overview, Performance, and First Results*, Publications of the Astronomical Society of the Pacific, 131:018002 (19pp), 2019 January

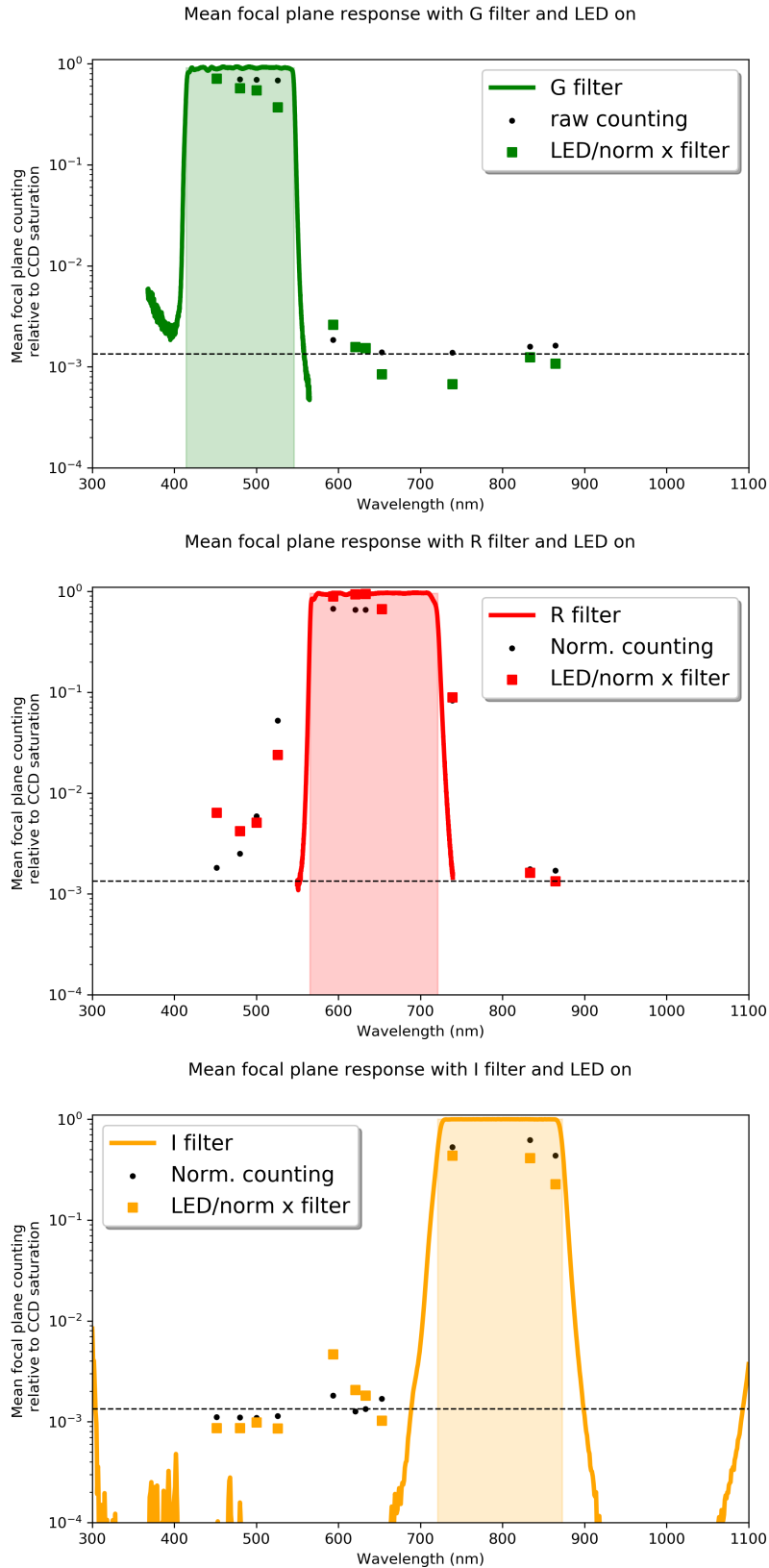


Figure 7: Normalized (to 2^{16}) mean focal plane counting (rectangle points) as a function of the LED peak wavelength with G filter (upper plot), R filter (middle plot) and I filter (lower plot). This relative counting is compared to the fraction of LED light inside the filter-band (black points). For each plot, the filter transmission (colored line) as well as its simple modeling (light-colored rectangle) are shown, but also the counting level obtained with LED "off" (dashed black line).

Focal plane response with G Filter to LED13

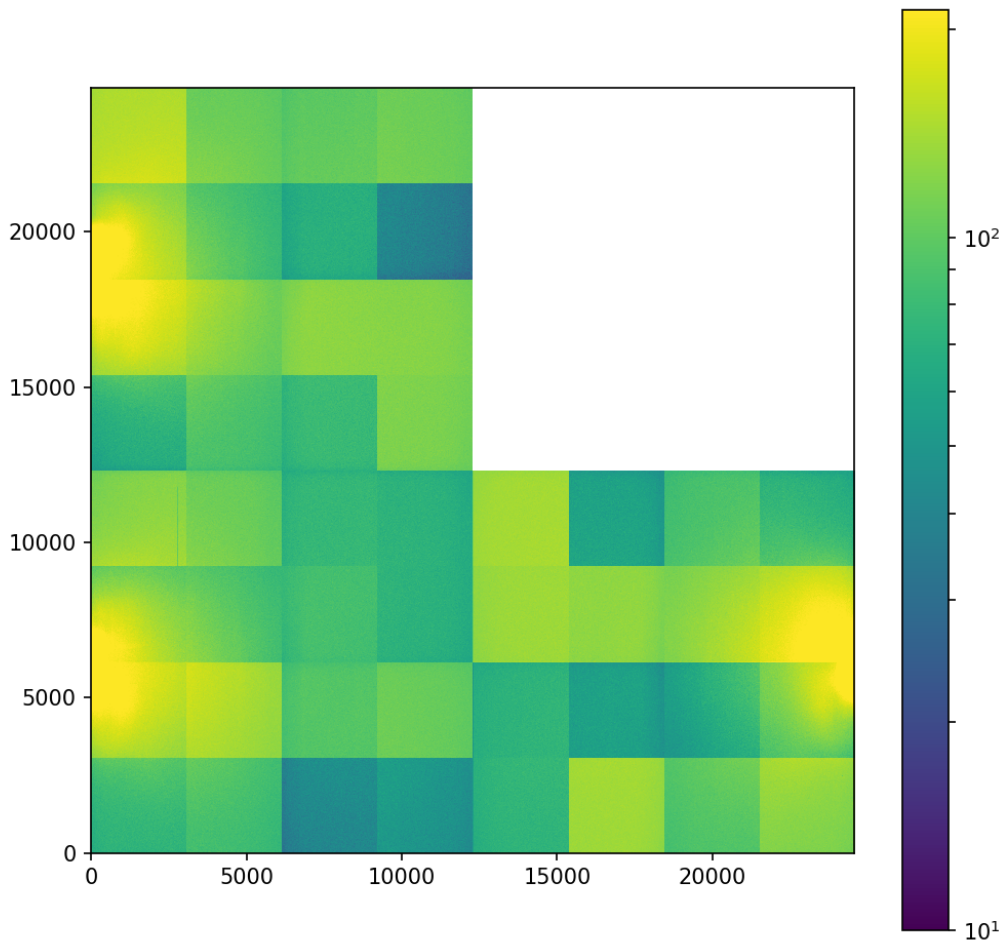
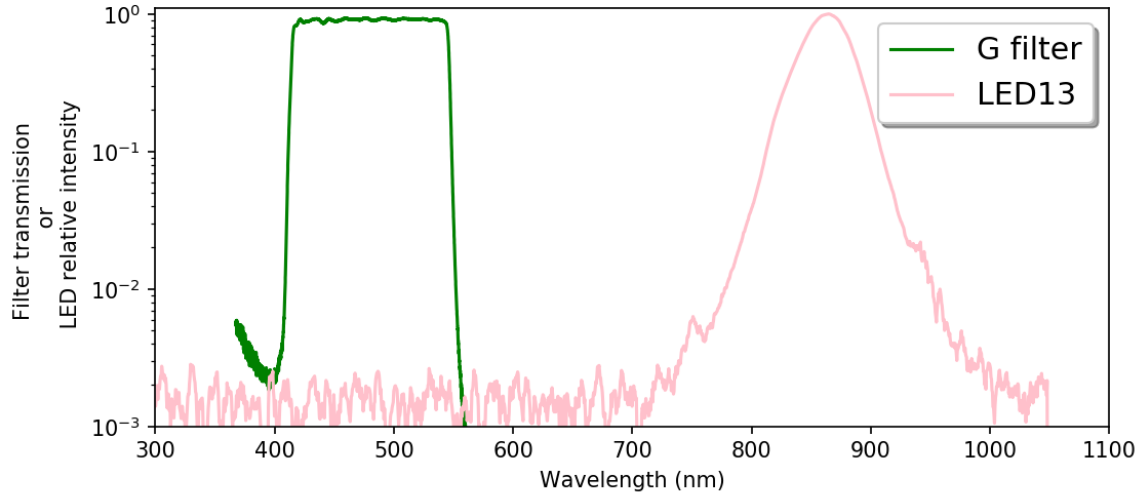


Figure 8: Full focale plane image with filter G illuminated by LED 13.

Focal plane response with G Filter to LED03

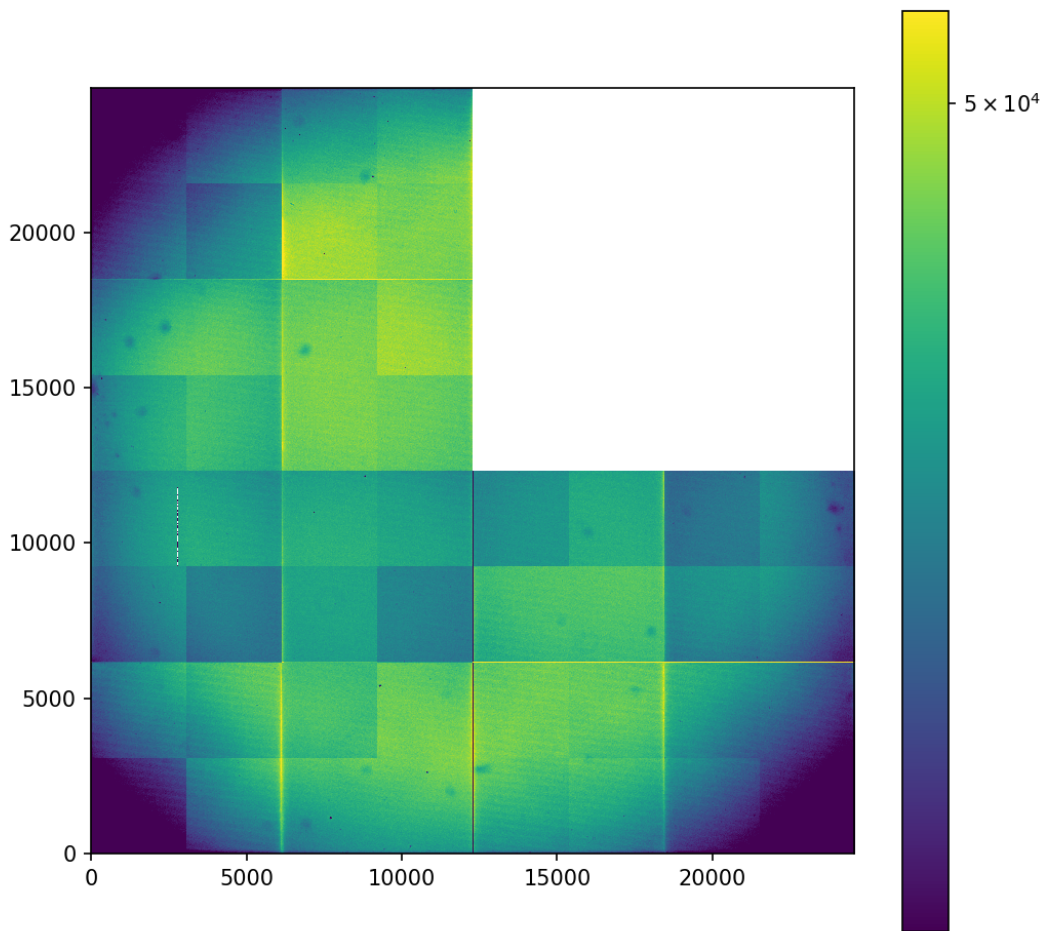
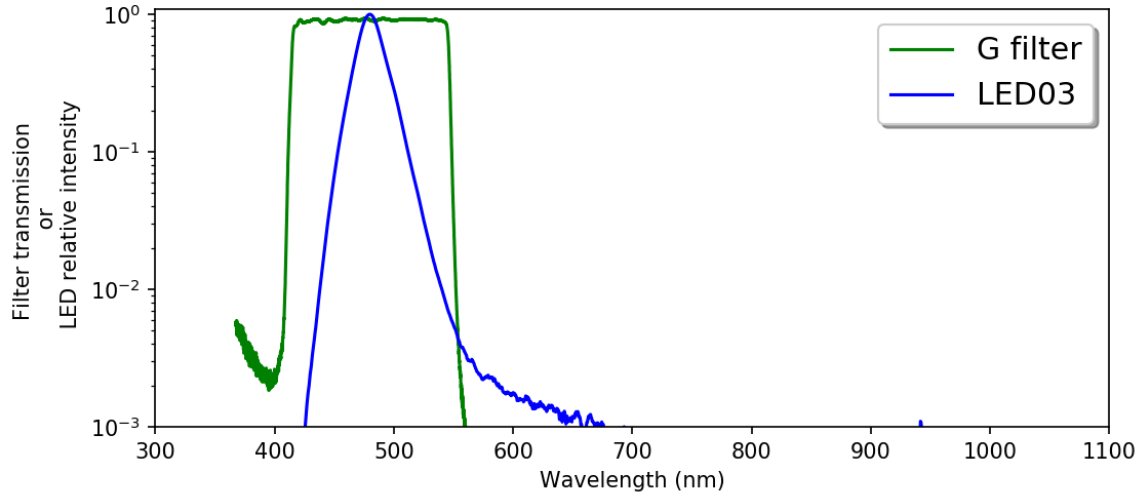


Figure 9: Full focal plane image with filter G illuminated by LED 03.

Focal plane response with R Filter to LED02

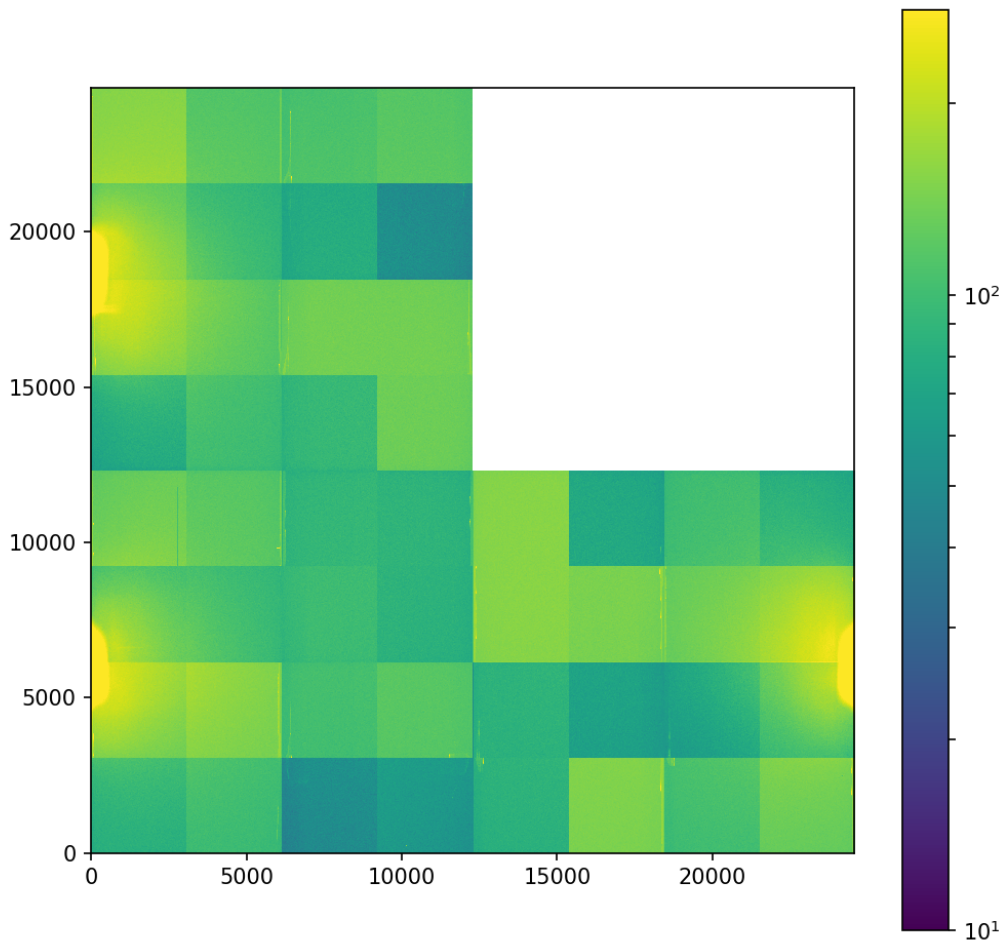
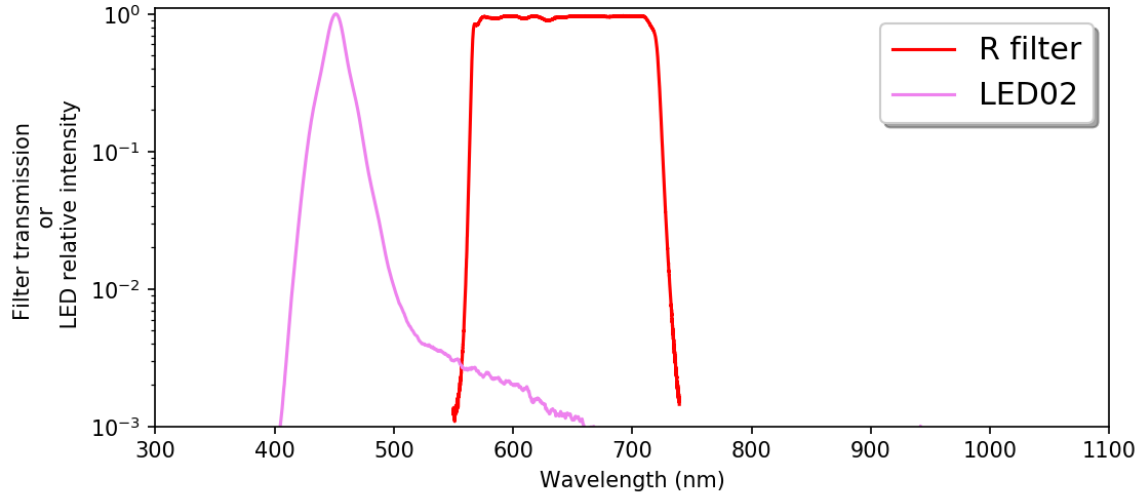


Figure 10: Full focal plane image with filter R illuminated by LED 02.

Focal plane response with R Filter to LED09

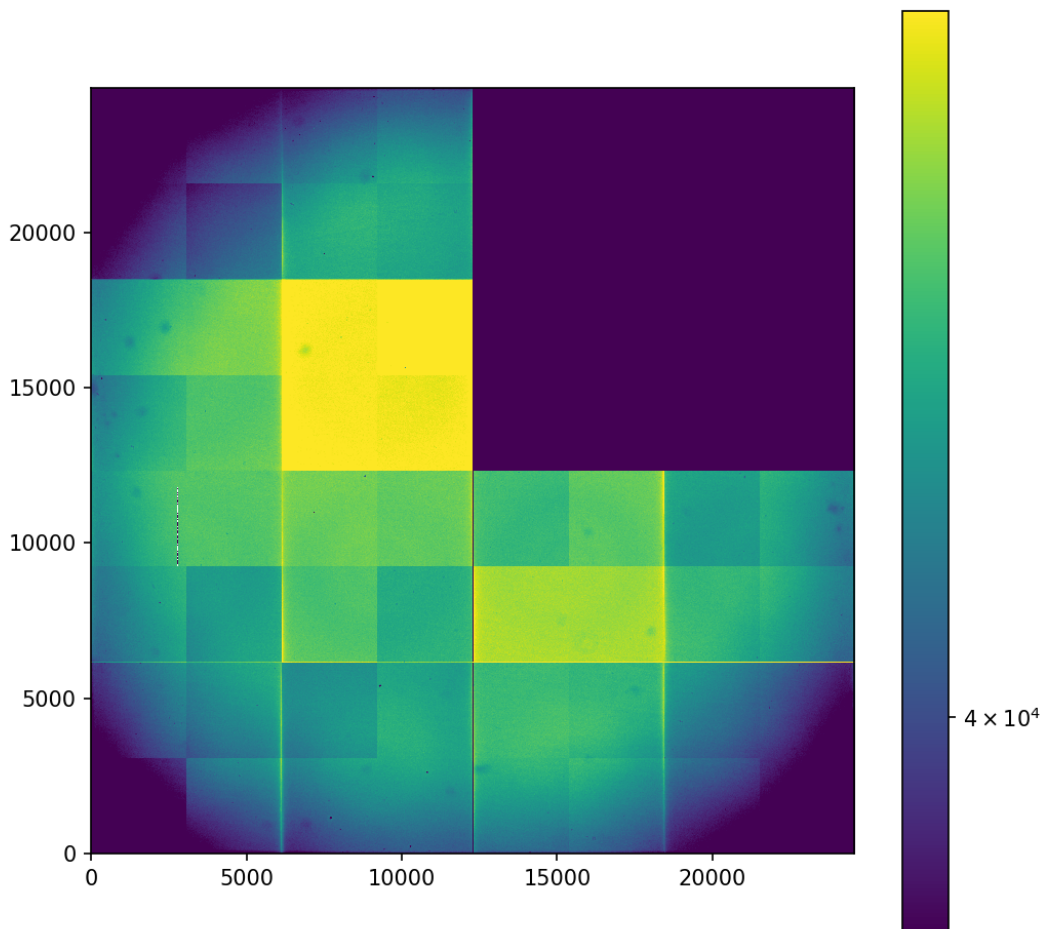
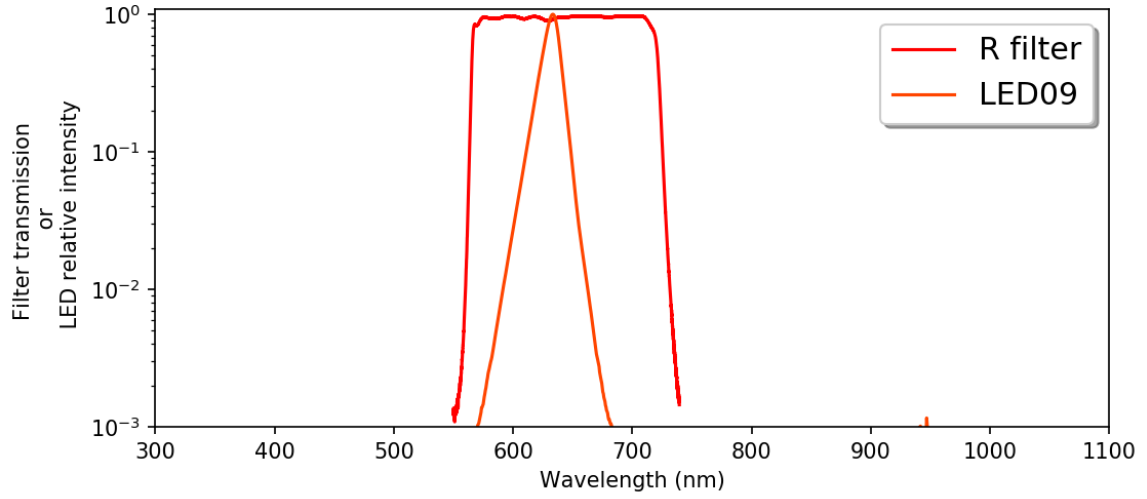


Figure 11: Full focale plane image with filter R illuminated by LED 09.

Focal plane response with I Filter to LED02

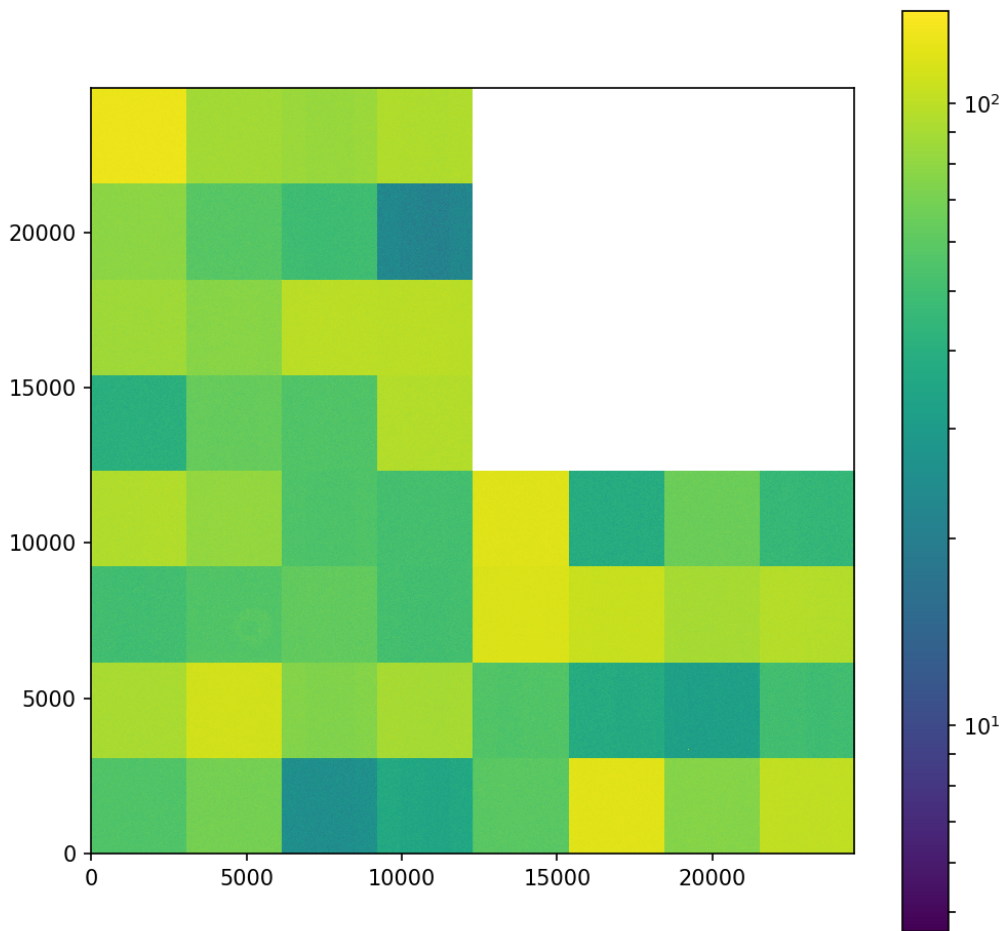
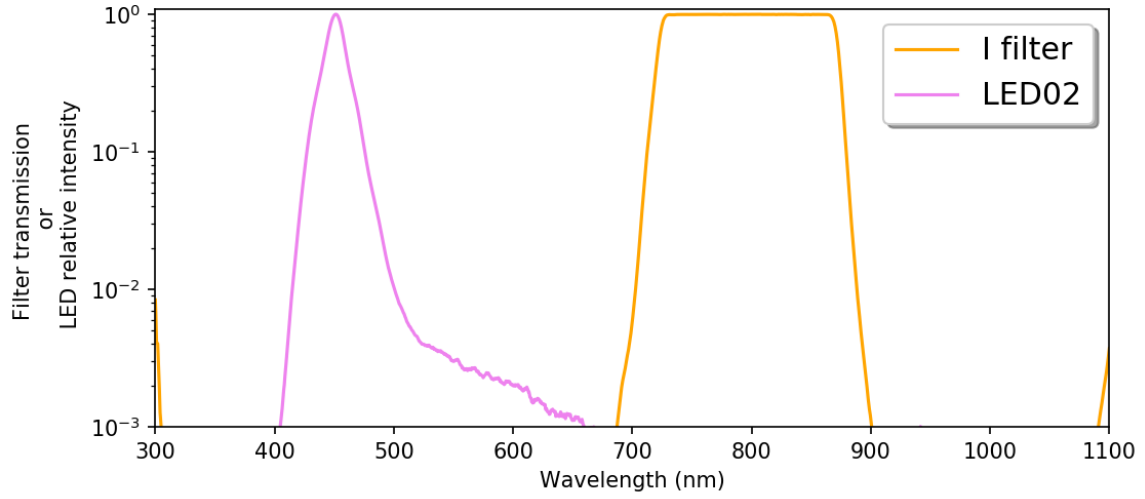


Figure 12: Full focale plane image with filter I illuminated by LED 02.

Focal plane response with I Filter to LED12

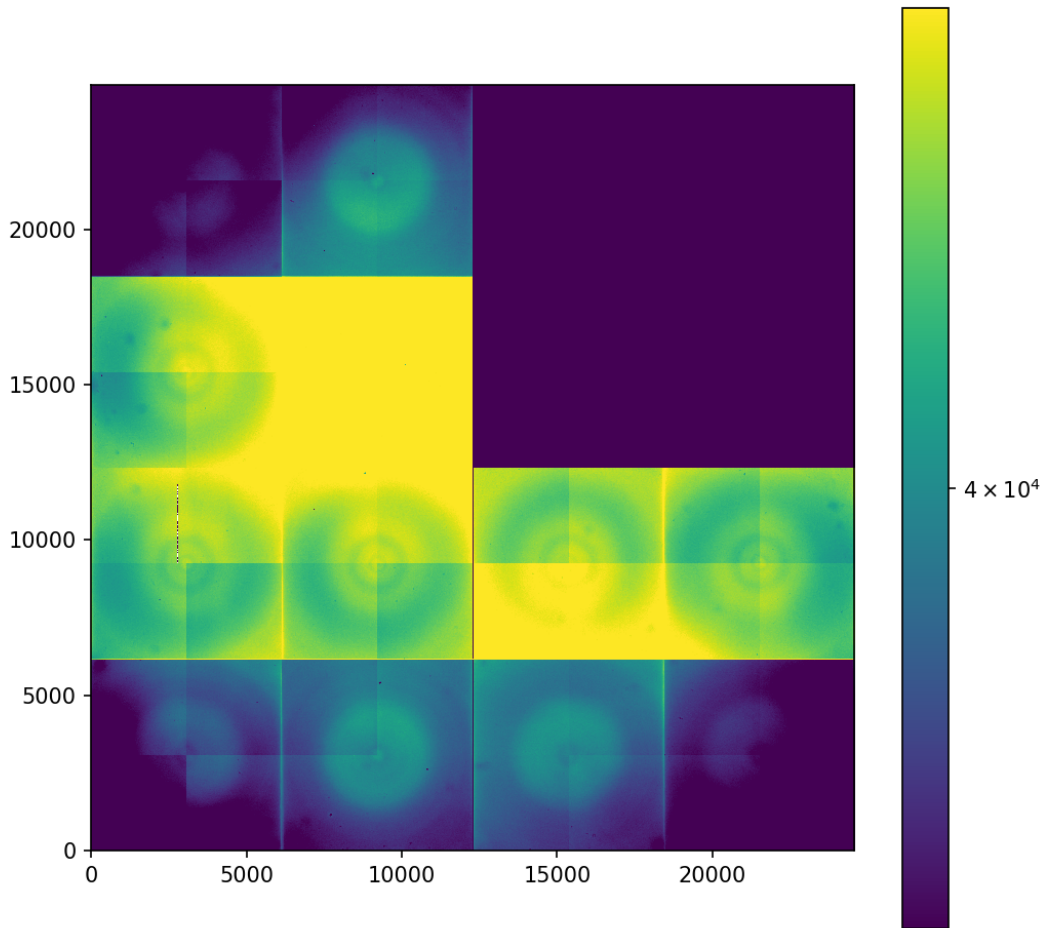
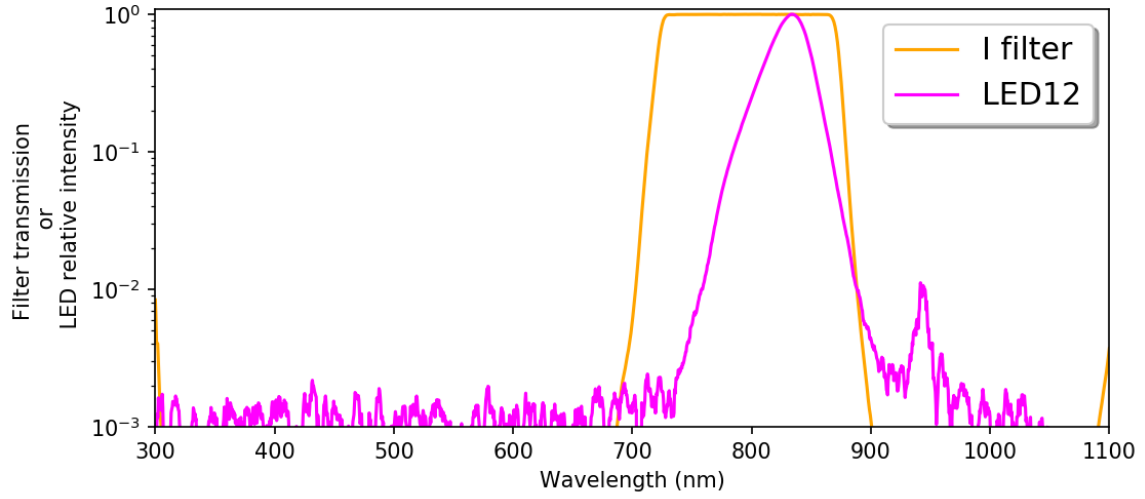


Figure 13: Full focale plane image with filter I illuminated by LED 12.

Focal plane response with G Filter to LED13

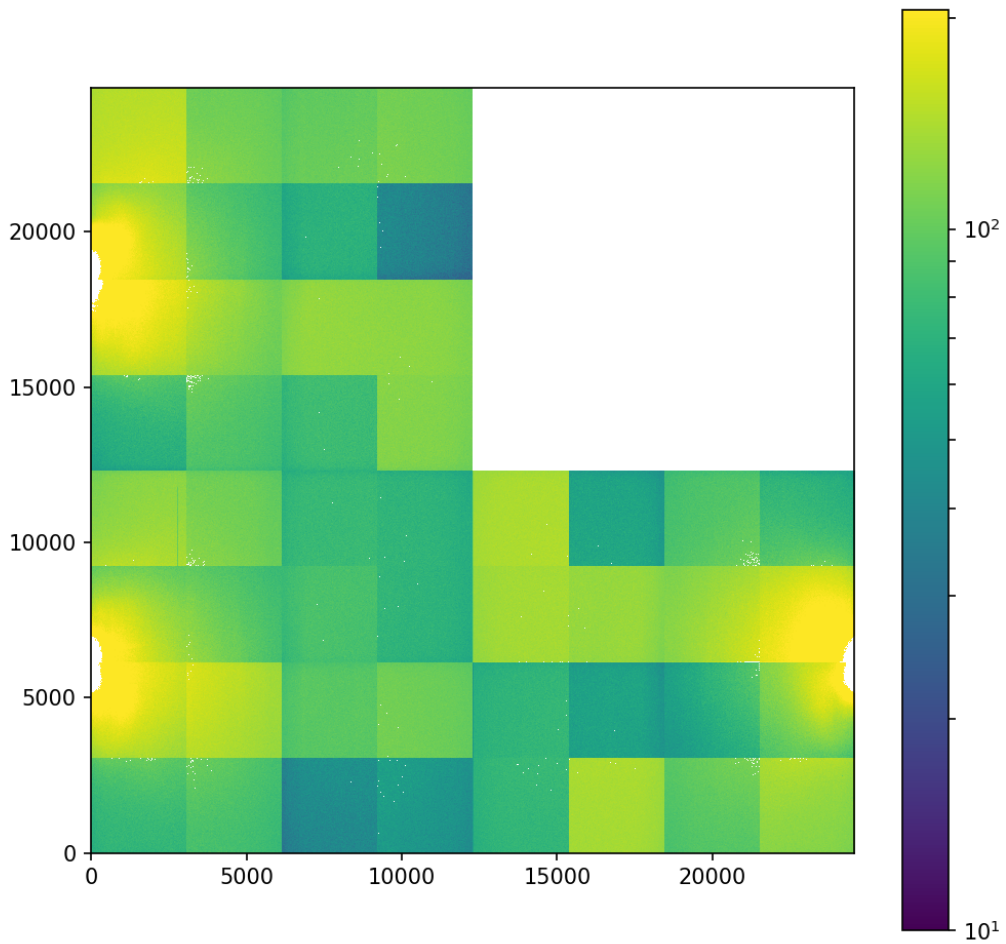
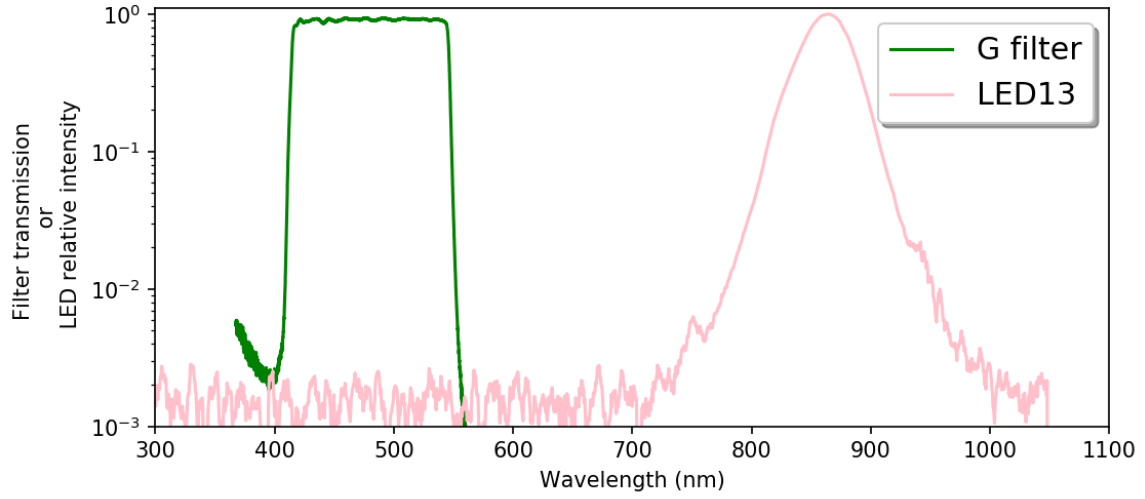


Figure 14: Full focal plane image with filter G illuminated by LED 13 after removal of pixels above threshold cut $n = 3$.

Focal plane response with G Filter to LED03

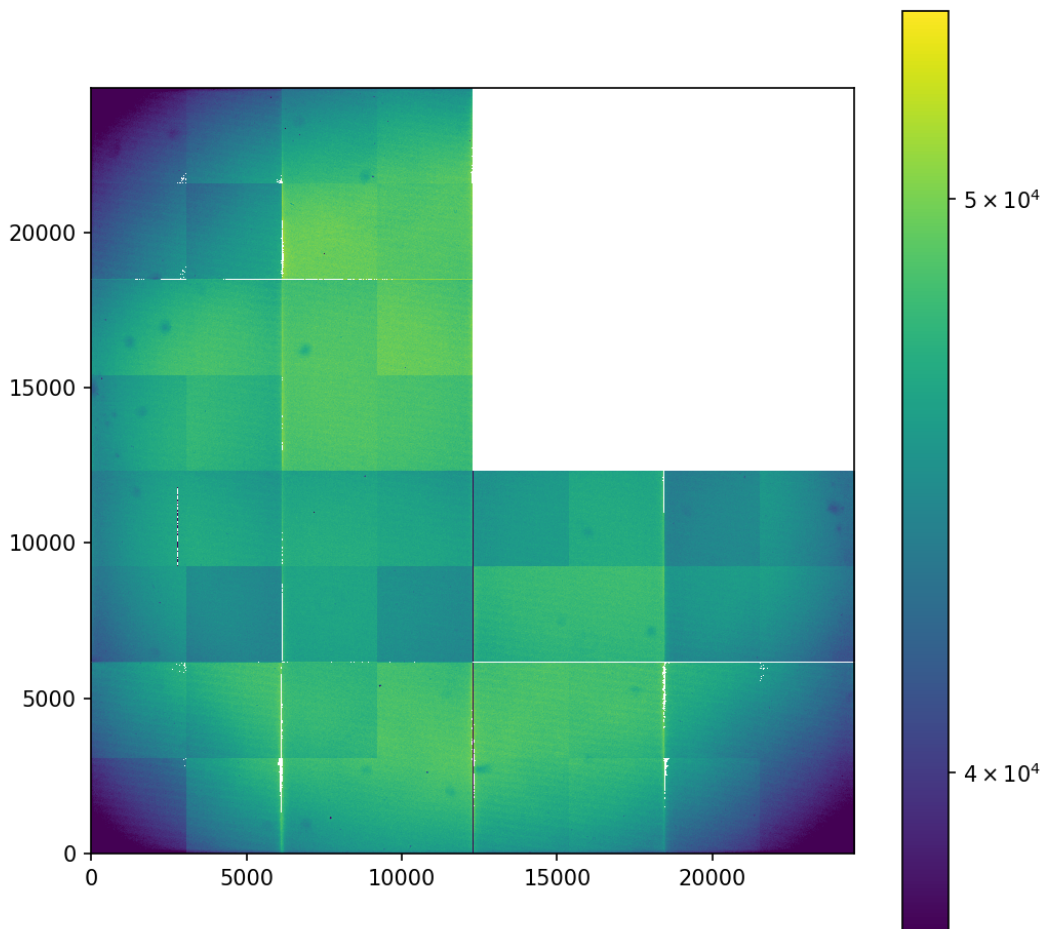
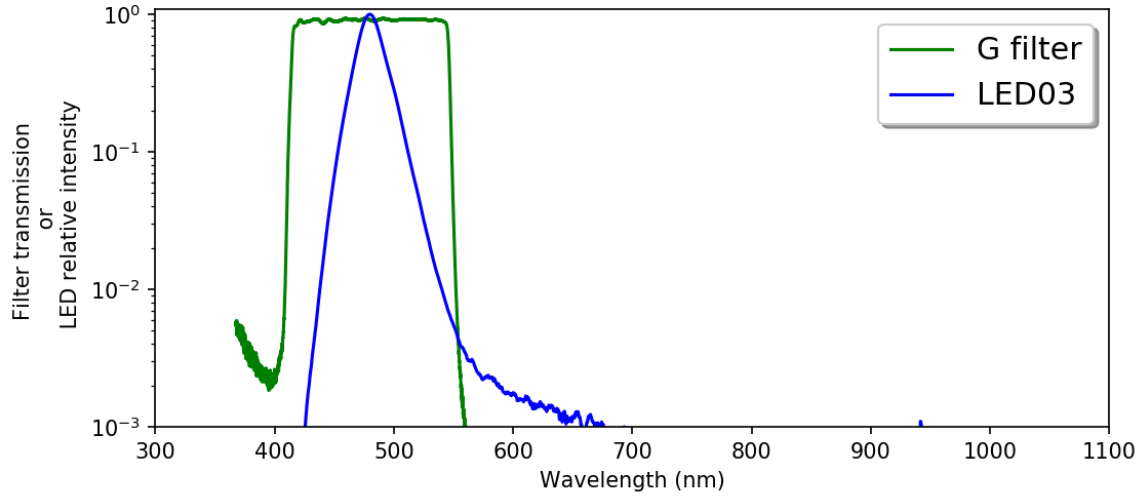


Figure 15: Full focal plane image with filter G illuminated by LED 03 after removal of pixels above threshold cut $n = 2$.

Focal plane response with R Filter to LED02

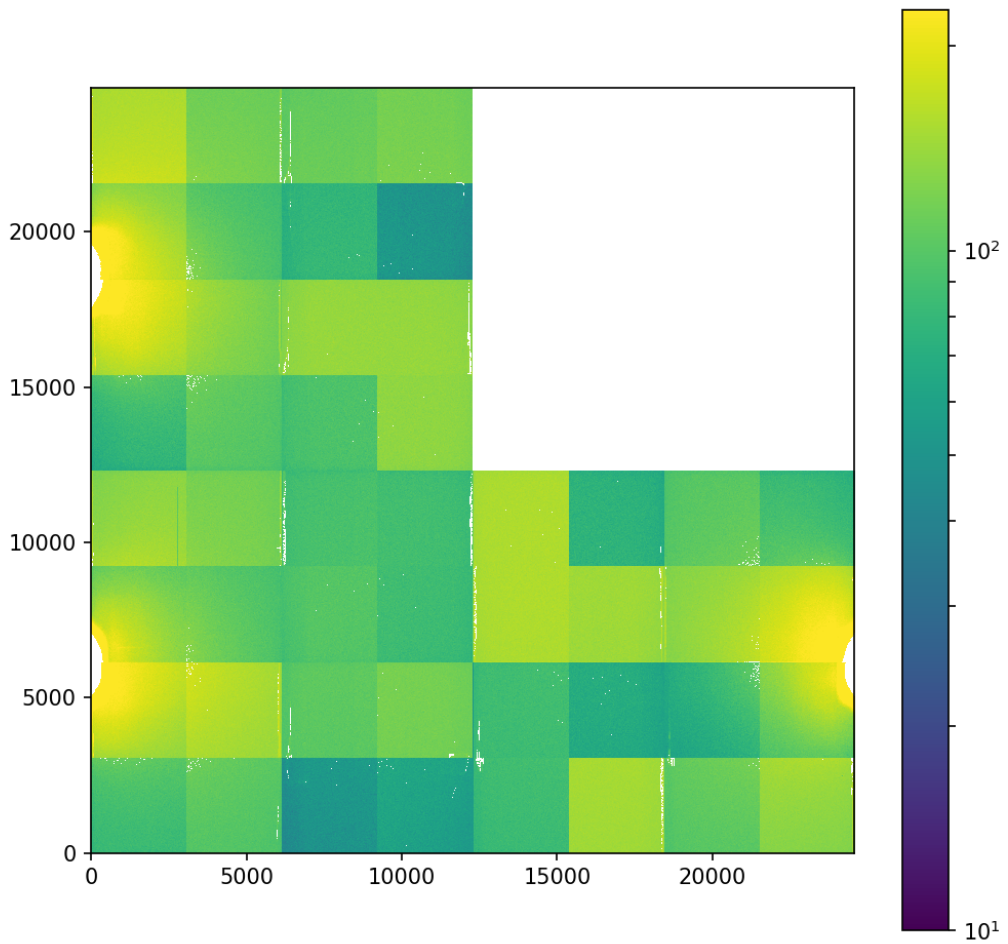
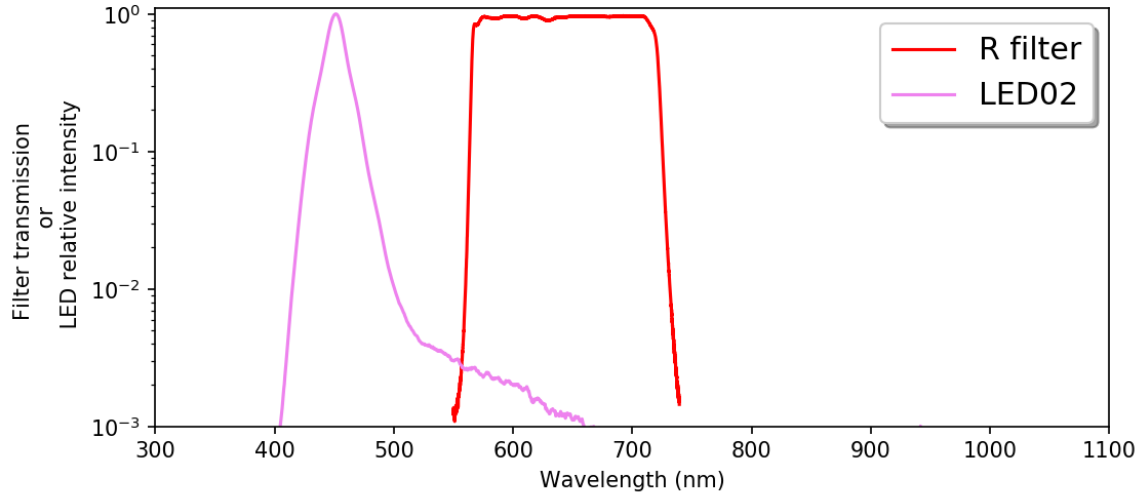


Figure 16: Full focale plane image with filter R illuminated by LED 02 after removal of pixels above threshold cut $n = 3$.

Focal plane response with R Filter to LED09

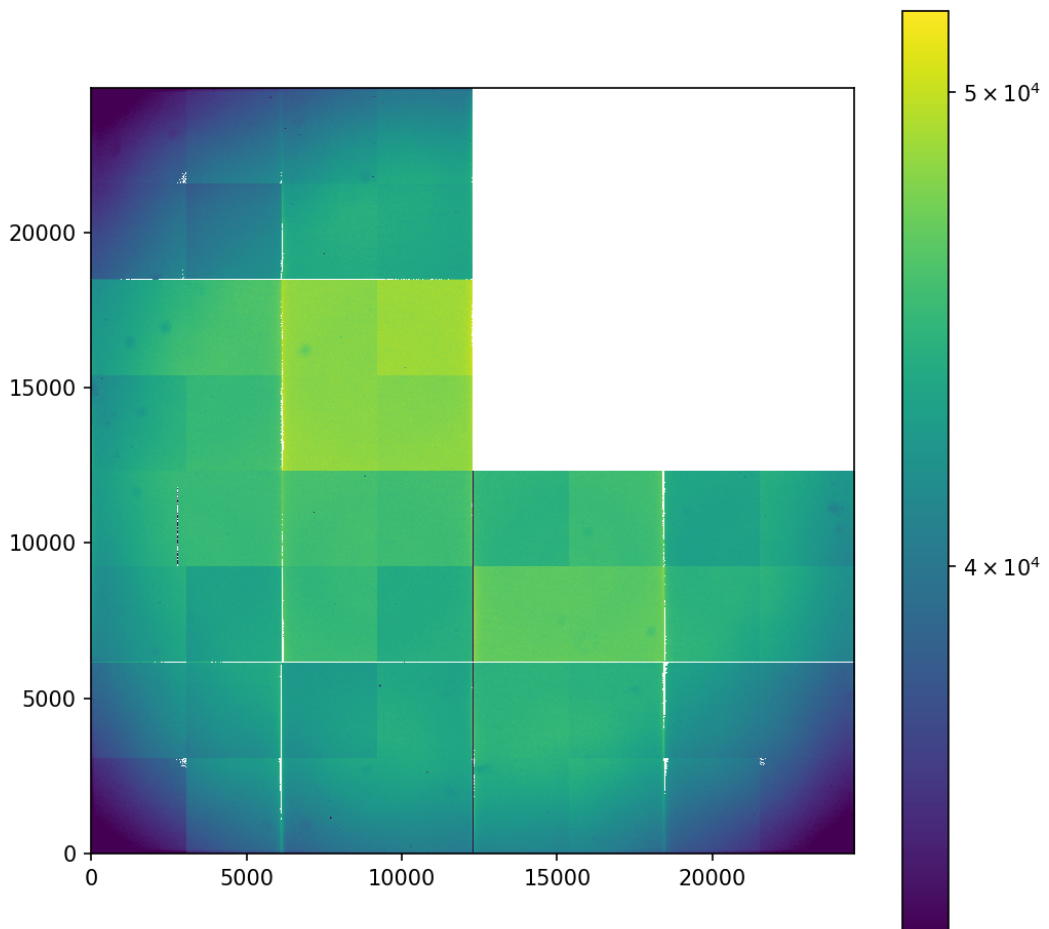
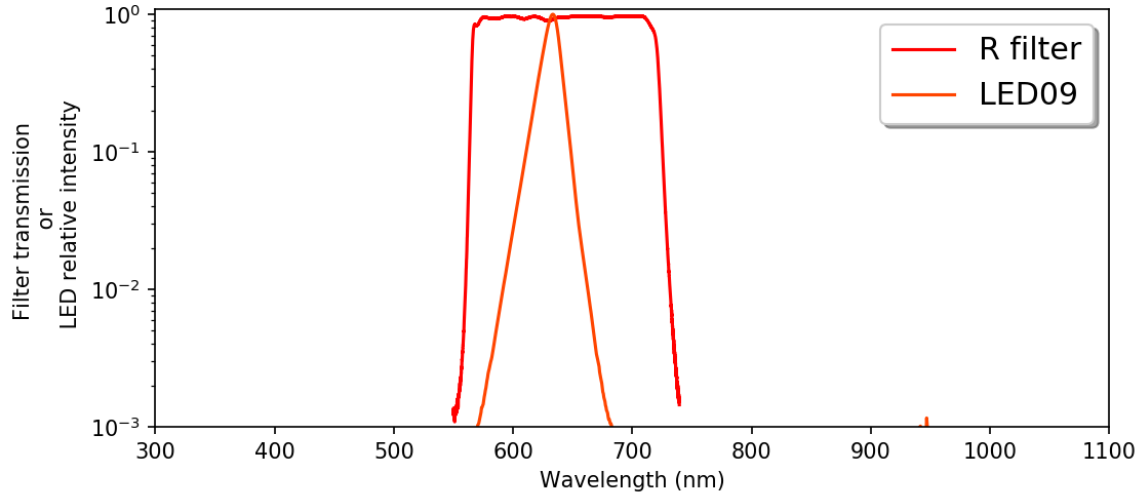


Figure 17: Full focal plane image with filter R illuminated by LED 09 after removal of pixels above threshold cut $n = 2$.

Focal plane response with I Filter to LED02

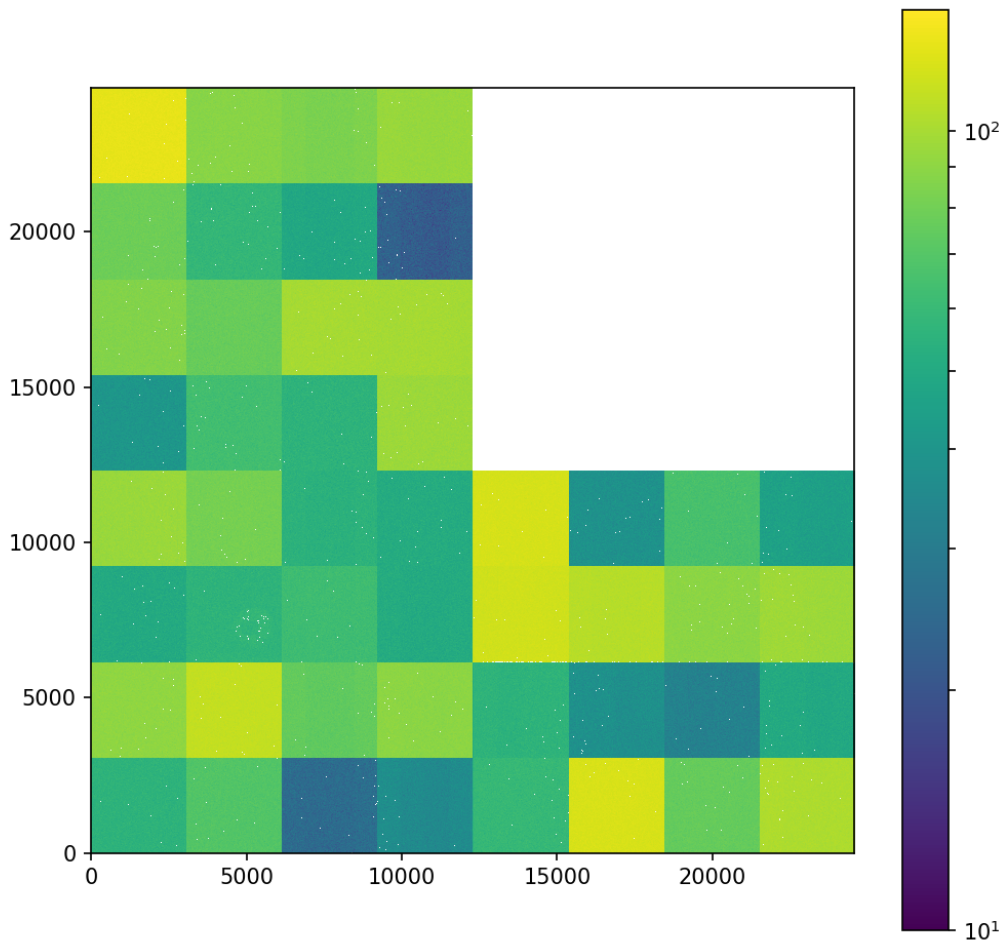
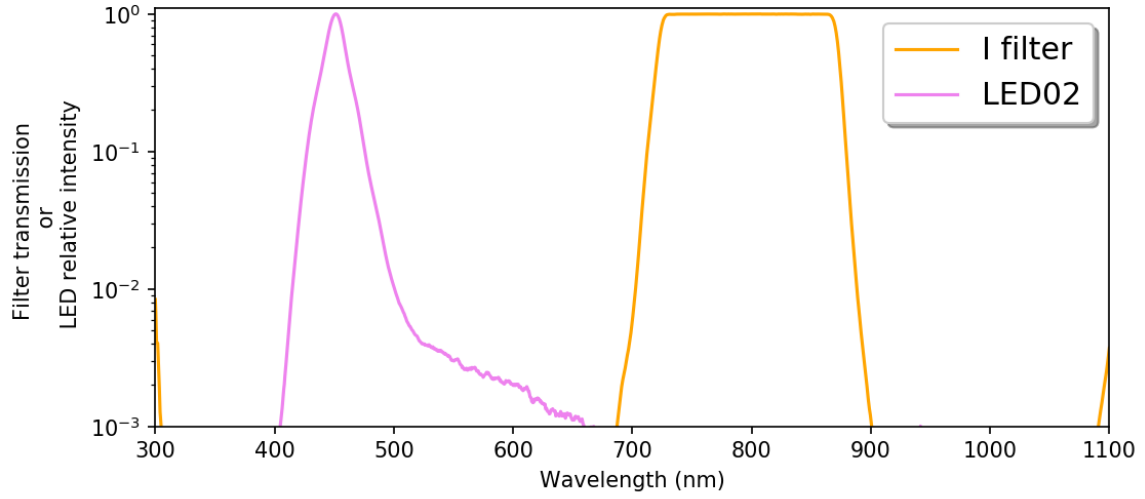


Figure 18: Full focale plane image with filter I illuminated by LED 02 after removal of pixels above threshold cut $n = 3$.

Focal plane response with I Filter to LED12

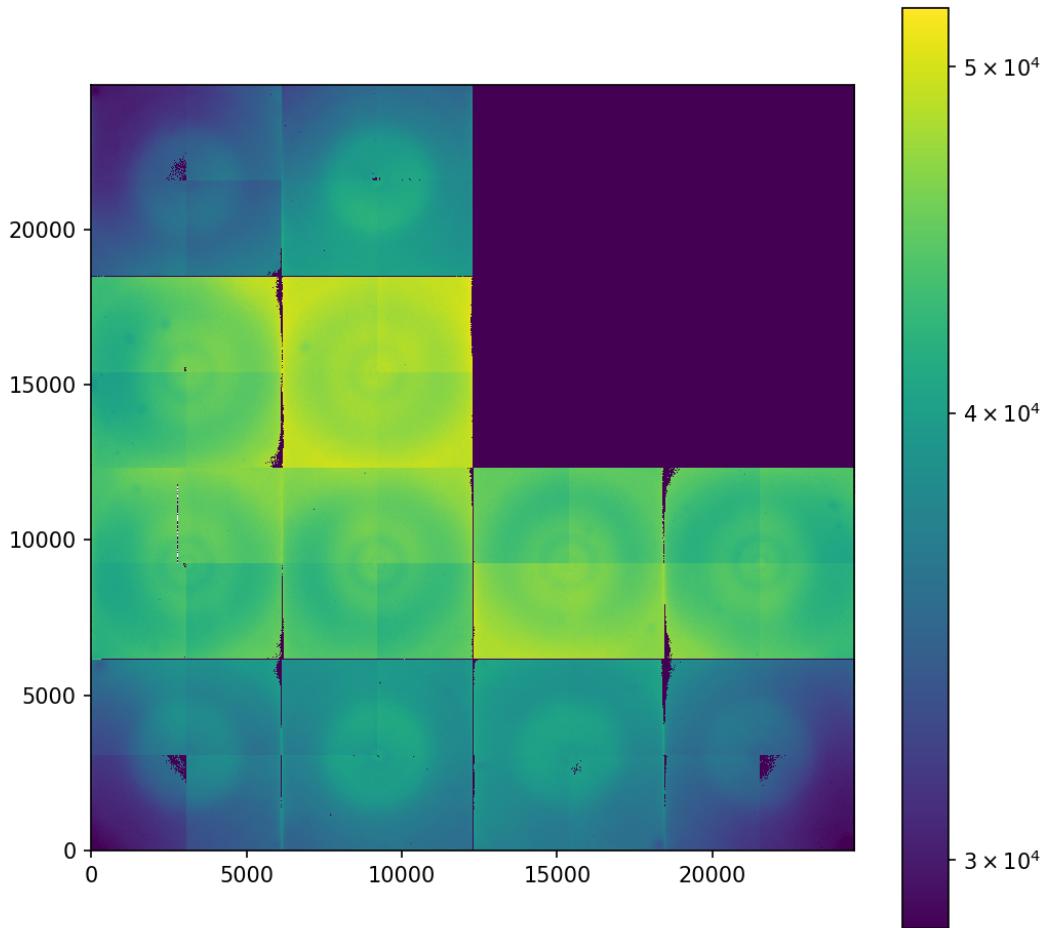
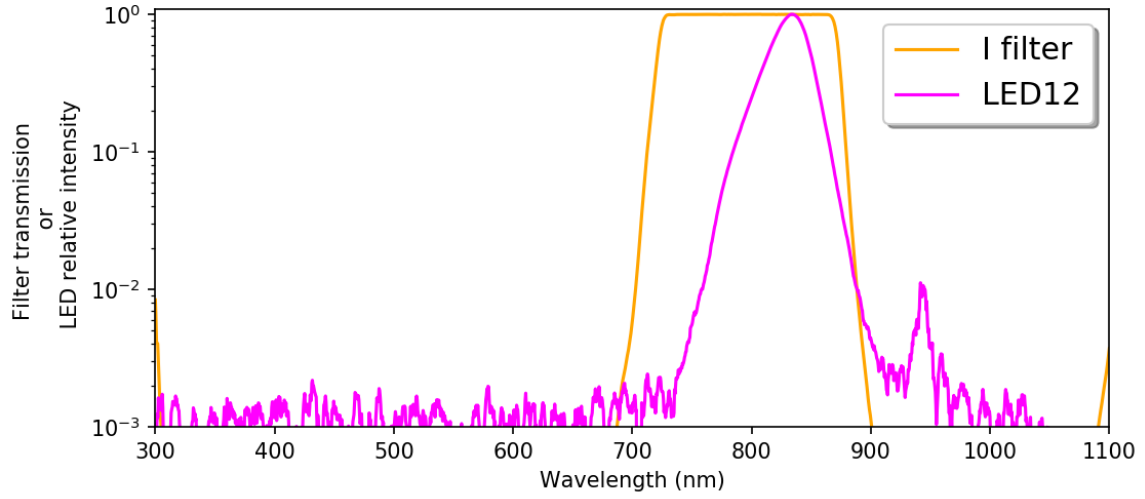


Figure 19: Full focal plane image with filter I illuminated by LED 12 after removal of pixels above threshold cut $n = 2$.